

MINISTRY OF EDUCATION  
AND TRAINING

VIETNAM ACADEMY OF  
SCIENCE OF TECHNOLOGY

**GRADUATE UNIVERSITY OF SCIENCE AND  
TECHNOLOGY**

---



**Pham Duy Binh**

**NUMERICAL STUDY OF COMPOUND LIQUID DROPLETS  
WITH PHASE CHANGE, HEAT TRANSFER**

Major: Fluid Mechanics  
Code number: 944 01 08

**SUMMARY OF DISSERTATION ON MECHANICS**

**Hanoi – 2023**

This work is completed at Graduate University of Science and Technology  
– Vietnam Academy of Science and Technology.

Scientific Supervisor 1: Assoc. Prof., Dr. Vu Van Truong

Scientific Supervisor 2: Assoc. Prof., Dr. Nguyen Thi Viet Lien

Reviewer 1:

Reviewer 2:

Reviewer 3:

This thesis was upheld at Scientific Council of Graduate University of  
Science and Technology – Vietnam Academy of Science and Technology  
at ..., day..., month..., 202...

This thesis is available at the following places:

- Library of Graduate University of Science and Technology
- National Library of Vietnam

## INTRODUCTION

### 1. The necessity of the dissertation

The compound droplet (i.e., compound liquid droplet) have great potential for applications in the manufacture of solar cells. There are many researchers interested in this renewable energy source because they are almost endless and cause less negative effects on the environment than fossil fuels. The component of the solar cell mentioned above consists of spherical semiconductor droplets placed in a grid. Accordingly, only a thin outer layer of the droplet is used in the conversion into electrical energy. Therefore, the use of hollow semiconductor droplets (or solidified compound droplet with gas cores) will help save semiconductors and make the semiconductor wafer lighter but still efficient. Studying the phase change of such semiconductor hollow droplets could make it possible to make mass-produced, cheaper and more widespread solar panels.

The study of phase change (in this thesis, solidification) of compound droplets also helps to find a solution to anti-icing on the surface of aircraft and wind turbine blades, improve machine life and efficiency. This ice phenomenon is common in a cold environment. Accordingly, water droplets in the air when in contact with the surface of the blades of an aircraft or an wind turbine will be frozen if the temperature at the blade surface is less than the solidification temperature of water. Such water droplets can mix with air bubbles inside, and they also freeze when attached to the blades. The freezing of water droplets on the blade surface can be a serious cause of reduced machine performance and life. More dangerous when it is

one of the causes in serious aviation accidents due to the impact on the aerodynamics of the air flow passing through the aircraft blades.

In addition, solidifying compound droplets are used to eliminate waste water, in the food industry and in the production of sound-absorbing materials.

Because of the potentials and applications of the above-mentioned solidified compound droplet, "*Numerical study of compound liquid droplets with phase change, heat transfer*" with the desire to control the solidification time and solidified droplet shape are chosen in this thesis. This study is expected to be applied in the production of solar cells and find solutions to improve machine efficiency and machine quality of aircraft and wind turbine blades.

## **2. The aims of the dissertation**

Studying the process of heat transfer, phase change (here is the solidification process) of a hollow fluid droplet (a type of the compound fluid droplet with a gas core inside) by front-tracking method.

## **3. The main content of the dissertation**

The main contents of the thesis include:

**Chapter 1:** An overview of compound droplet dynamics

**Chapter 2:** Investigation and building a computation program for the problem of heat transfer, phase change

**Chapter 3:** Studying the process of heat transfer, phase change of a hollow fluid droplet on a cold surface

**Chapter 4:** Studying the process of heat transfer and phase change of a suspended hollow fluid droplets under the forced convection

Finally, the conclusion section summarizes the results achieved in this thesis and issues to be solved in the future.

## **CHAPTER 1. AN OVERVIEW OF COMPOUND DROPLET DYNAMICS**

In this chapter, some concepts are presented such as compound droplet, hollow droplet, phase change of a fluid droplet,... and show some of the key dimensionless parameters used in the thesis. The thesis also proposes two methods to create a compound droplet: the compound droplet separation of fluid jet and the compound droplet separation of fluid filament. Some typical applications of compound droplets are also presented such as applications in food technology, biomedical technology, in manufacturing sound-absorbing materials,... Especially in the manufacturing industry of solar cells and improve engine efficiency, anti-icing from the surface of aircraft and wind turbine blades.

Through surveying the studies on solidification of fluid droplets, the following conclusions are drawn:

- There are many researchers interested in and building theoretical solidification models of fluid droplets. However, the these studies only focused on the solidification of simple droplets. Research works for compound droplets are lacking.

- Experimental studies on solidification of simple droplets are numerous, but research on hollow droplets has only a few done.
- Investigation on phase change of hollow droplets by simulation method has not been done up to now. This leads to the birth of this topic.

Finally, a numerical method is chosen to simulate the solidification of hollow droplets. Common methods used to simulate the phase change of a fluid droplet include the level-set method, the volume of fluid method, the lattice Boltzmann method, and the front-tracking method. In this thesis, the front-tracking method is chosen to simulate the phase change of hollow droplets because of its advantages such as accurate and simple boundary approximation, accurate surface tension computation.

## **CHAPTER 2. INVESTIGATION AND BUILDING A COMPUTATION PROGRAM FOR THE PROBLEM OF HEAT TRANSFER, PHASE CHANGE**

In this chapter, the thesis focuses on building a simulation program for a liquid droplet with heat transfer, phase change. The fluids in the problems in the thesis are assumed to be incompressible, immiscible and Newtonian. The systems of equations used in the thesis are:

- Navier-Stokes equation

$$\begin{aligned} \frac{\partial \rho \mathbf{u}}{\partial t} + \nabla \cdot \rho \mathbf{u} \mathbf{u} = -\nabla p + \nabla \cdot \left[ \mu (\nabla \mathbf{u} + \nabla \mathbf{u}^T) \right] \\ + \int_f \sigma \kappa \delta(\mathbf{x} - \mathbf{x}_f) \mathbf{n}_f \cdot dS + \rho(\mathbf{f} + \mathbf{g}) \end{aligned} \quad (2.1)$$

- Energy equation

$$\frac{\partial (\rho C_p T)}{\partial t} + \nabla \cdot (\rho C_p T \mathbf{u}) = \nabla \cdot (k \nabla T) + \int_f \dot{q} \delta(\mathbf{x} - \mathbf{x}_f) \cdot dS \quad (2.2)$$

- Heat flux on the solidifying front

$$\dot{q} = k_s \left. \frac{\partial T}{\partial n} \right|_s - k_l \left. \frac{\partial T}{\partial n} \right|_l \quad (2.3)$$

Due to the difference in densities between the solid and liquid phases, the continuity equation is

$$\nabla \cdot \mathbf{u} = \frac{1}{L_h} \left( \frac{1}{\rho_s} - \frac{1}{\rho_l} \right) \int_f \delta(\mathbf{x} - \mathbf{x}_f) \dot{q} dS \quad (2.4)$$

Dimensionless parameters appear when we normalize Navier-Stokes equation and the energy equation. In addition, several other dimensionless parameters such as the ratios of the phase properties, and the geometry of the hollow liquid droplet are also used. The dimensionless parameters used in the thesis are

$$\begin{aligned} Pr = \frac{C_{pl} \mu_l}{k_l}, St = \frac{C_{pl} (T_m - T_c)}{L_h}, Bo = \frac{\rho_l g R^2}{\sigma}, \\ Oh = \frac{\mu_l}{\sqrt{\rho_l R \sigma}}, We = \frac{\rho_l U_i^2 R}{\sigma}, Re = \frac{\rho_l U_i R}{\mu_l}, \end{aligned} \quad (2.5)$$

$$\theta_0 = \frac{T_0 - T_c}{T_m - T_c}, \rho_{sl} = \frac{\rho_s}{\rho_l}, \rho_{gl} = \frac{\rho_g}{\rho_l}, \mu_{gl} = \frac{\mu_g}{\mu_l}, R_{io} = \frac{R_i}{R_o} \quad (2.6)$$

$$k_{sl} = \frac{k_s}{k_l}, k_{gl} = \frac{k_g}{k_l}, C_{psl} = \frac{C_{ps}}{C_{pl}}, C_{pgl} = \frac{C_{pg}}{C_{pl}}, \varepsilon_0 = \frac{z_{ci0} - z_{co0}}{R} \quad (2.7)$$

In which,  $Pr$  is the Prandtl number that characterizes the ratio of momentum diffusion to thermal diffusion.  $St$  is the Stefan number representing the ratio of the characteristic heat to the latent heat of fusion.  $Bo$  is the Bond number representing the ratio of gravity to surface tension.  $We$  is the Weber number representing the inertial force relative to the surface tension.  $\theta_0$  is the initial dimensionless temperature.  $\rho_{sl}$ ,  $\rho_{gl}$  are density ratios,  $\mu_{gl}$  is the viscosity ratio,  $R_{io}$  is the ratio of the radii between the inner and outer droplets.  $k_{sl}$ ,  $k_{gl}$  is the ratios of thermal conductivities,  $C_{psl}$ ,  $C_{pgl}$  is the ratios of heat capacities.  $\varepsilon_0$  is the initial eccentricity between the inner and outer droplets. For hollow liquid droplets, we choose the outer radius as the base, i.e.,  $R = R_o$ .

The Navier-Stokes and energy equations are discretized to be included in the computational program.

First, we separate the Navier-Stokes equation (2.1) into two equations

- The equation with pressure component

$$\frac{\mathbf{u}^{n+1} - \mathbf{u}^*}{\Delta t} = -\frac{\nabla_h p}{\rho^n} \quad (2.8)$$

- The equation has no pressure component



$$\frac{\mathbf{u}^* - \mathbf{u}^n}{\Delta t} = -\nabla \cdot (\mathbf{u}\mathbf{u})^n + \frac{1}{\rho^n} \left\{ \nabla \cdot \left[ \mu (\nabla \mathbf{u} + \nabla \mathbf{u}^T) \right] + \int_f \sigma \kappa \delta (\mathbf{x} - \mathbf{x}_f) \mathbf{n}_f \cdot dS \right\}^n + (\mathbf{f} + \mathbf{g})^n \quad (2.9)$$

We take the divergence operator (div operator) on both sides of equation (2.8)

$$\nabla_h \cdot \left( \frac{1}{\rho^n} \nabla_h p \right) = \frac{1}{\Delta t} (\nabla_h \cdot \mathbf{u}^* - \nabla_h \cdot \mathbf{u}^{n+1}) \quad (2.10)$$

The temporary velocity  $\mathbf{u}^*$  is found in equation (2.9), followed by the pressure in equation (2.10). Finally the velocity at the next step is found through equation (2.8).

After finding the velocity and pressure. We proceed to discrete energy equation (2.2)

$$\frac{C_p^n (T^{n+1} - T^n)}{\Delta t} = -\nabla \cdot (C_p T \mathbf{u})^n + \frac{1}{\rho^n} \left[ \nabla \cdot (k \nabla T)^n + \left( \int_f \dot{q} \delta (\mathbf{x} - \mathbf{x}_f) \cdot dS \right)^n \right] \quad (2.11)$$

A algorithm diagram (*Figure 2.1*) is built to help us visualize the computational processes of the program in time steps. Accordingly, variables such as density ( $\rho$ ), velocity ( $\mathbf{u}$ ), pressure ( $p$ ), temperature ( $T$ ), ... are updated through each corresponding loop.

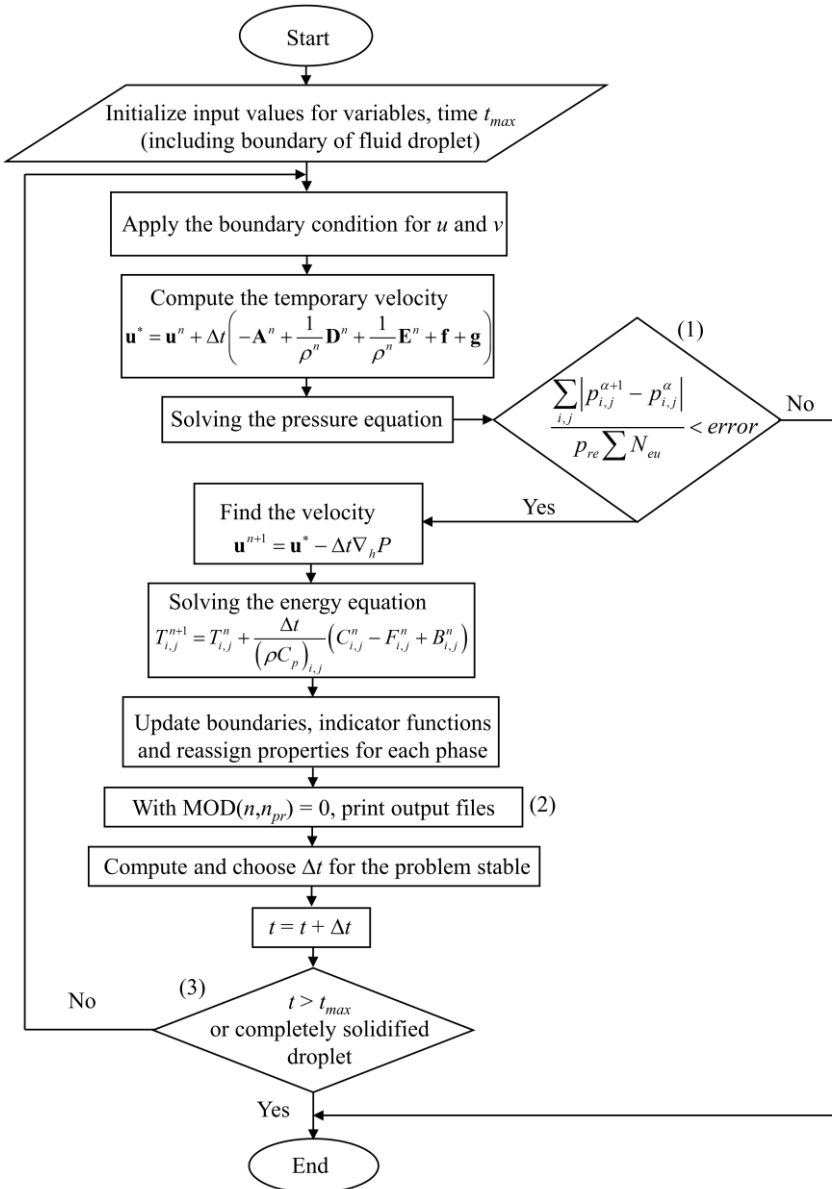


Figure 2.1. Algorithm diagram

The thesis uses front-tracking method to simulate the phase change problem. Accordingly, the interfaces are represented by interconnected series of points and they move in a fixed grid. Accordingly, each time step the coordinates of those points are updated according to

$$\mathbf{x}_f^{n+1} = \mathbf{x}_f^{n+1} + \mathbf{V}_f \Delta t \quad (2.12)$$

For  $t$  and  $t + \Delta t$ , respectively, the computation steps  $n$  and  $n + 1$ . The velocity of the interfaces  $\mathbf{V}_f$  is interpolated from the four nearest grid points or the heat balance condition at the solidifying front. The properties of the phases specified by the two indicator functions  $I_1$  and  $I_2$  are reconstructed from the position of the interfaces. The indicator functions have a value of 1 in this phase and 0 in the other phases. We denote the properties of the phases such as density ( $\rho$ ), viscosity ( $\mu$ ), heat capacity ( $C_p$ ) and thermal conductivity ( $k$ ) as  $\varphi$

$$\varphi = [\varphi_s I_1 + \varphi_l (1 - I_1)] I_2 + \varphi_g (1 - I_2) \quad (2.13)$$

Unlike the solidification problem of simple liquid droplets, hollow liquid droplets have two triple points. The growth angle at these triple points is assumed to be calculated as follows

$$\phi_{gr} = \phi_s - \phi_l \quad (2.14)$$

To verify the computational program just built, the simulation results of simple droplets ( $R_{io} = 0$ ) solidifying on the cold surface have a good agreement with the experimental datas of Pan et al., and Huang et al., (the problem model can be seen in *Figure 2.2*).

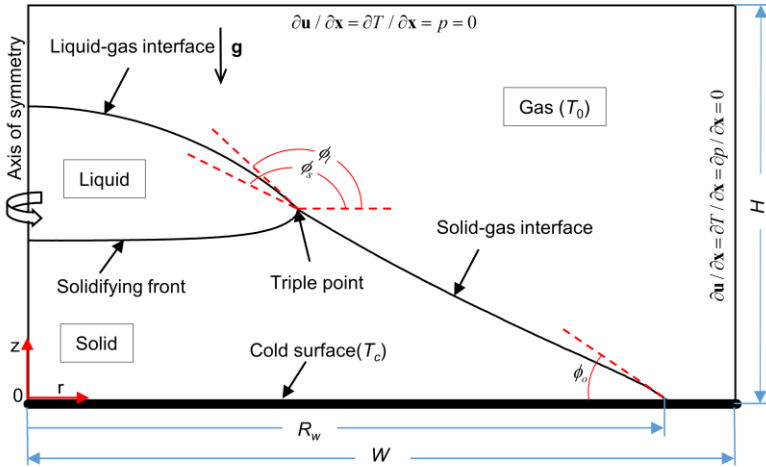


Figure 2.2. Solidification of a simple droplet on a cold flat surface with the computational domain  $W \times H$  and the wetting radius  $R_w$

Therefore, it shows that the computational program has high reliability and can be used to study the process of heat transfer and phase change of hollow liquid droplets.

## Conclusion of chapter 2

In this chapter, a computational program for a fluid droplet with heat transfer, phase change is built. Accordingly, the two Navier-Stokes and the energy equations have been discretized to be included in the computational program.

The front-tracking method is used to study the problem of heat transfer and phase change of a fluid droplet. Accordingly, the interfaces between the phases are modeled as a series of points. Each step of computing, these points moves and is updated again. Two

indicator functions  $I_1$  and  $I_2$  are used to determine the phase properties at every point on the computational domain.

The numerical simulation results have a good agreement with the experimental datas. Therefore, it shows that the computational program has high reliability and can be used to study the process of heat transfer and phase change of hollow liquid droplets.

*The results of comparing the computational program with experimental works have been published in a domestic journal, specifically, the paper number 6 in the "List of author's scientific works relating to the content of the dissertation"*

### **CHAPTER 3. STUDYING THE PROCESS OF HEAT TRANSFER, PHASE CHANGE OF A HOLLOW DROPLET ON A COLD SURFACE**

A number of experimental works have monitored the solidification of hollow liquid droplets such as the work of Vu et al., and Bahgat et al., These experimental works all use a pair of coaxial nozzles to create a hollow liquid droplet. This droplet can solidify during falling (not yet in contact with a cold surface) or after contact with a certain cold surface. This chapter focuses on simulating the second case that is "*hollow droplets solidify after contact with a cold surface*".

The model of the problem of a hollow droplet solidifying on a cold surface is presented in *Figure 3.1*. The cold surface is kept at a fixed temperature  $T_c$ . The problem consists of three incompressible,

immiscible, and Newtonian phases: solid (with density  $\rho_s$ ), liquid (with density  $\rho_l$  and viscosity  $\mu_l$ ) and gas (with density  $\rho_g$  and viscosity  $\mu_g$ ).

Initially, the hollow droplet consists of a liquid shell (outer droplet) covering a gas bubble core (inner droplet) that was assumed to be a hemisphere. The gas surrounding the droplet is assumed to have the same properties as the gas bubble core. Therefore, the liquid phase of the hollow droplet is the liquid shell between the inner and outer gaseous layers, and thus the phase change occurs only in the liquid shell of the hollow droplet. Several previous studies have investigated and simulated simple droplet solidifying on a cold

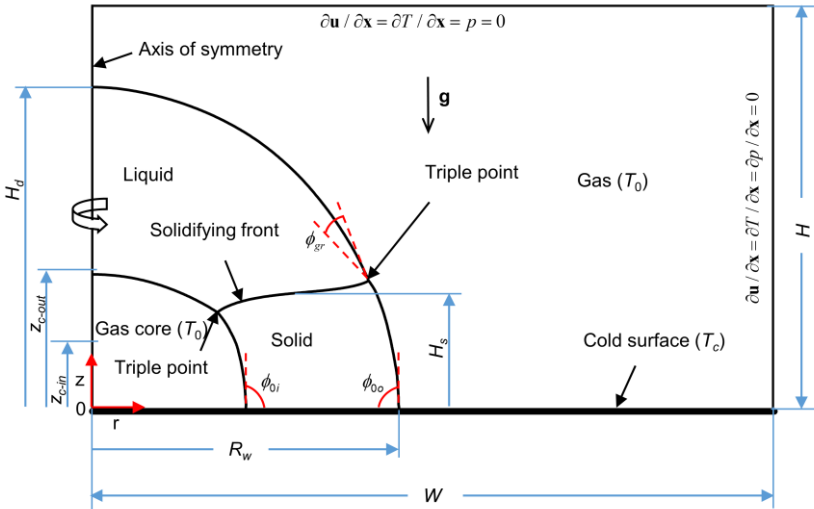


Figure 3.1. Symmetrical hollow droplet solidifying on a cold surface held at temperature  $T_c$ .  $z_{c-in}$  and  $z_{c-out}$  are the coordinates of the centroids of the inner and outer droplets

surface showing that the initial shape of droplet is assumed to be part of the sphere at the beginning of the simulation. Therefore, at time  $t = 0$ , the initial hollow droplet assumes to have a spherical shape in this study is acceptable. The initial equivalent radii of the outer and inner droplets are  $R_o$  and  $R_i$ , respectively. The liquid phase has a higher temperature  $T_m$  than the solidification temperature  $T_c$ . Thus, solidification begins at the surface of the cold plate and grows upward of the droplet. During solidification, the solid phase (denoted by subscript  $s$ ), liquid phase (denoted by subscript  $l$ ) and gas phase (denoted by subscript  $g$ ) intersect at the triple line (in this study is a triple point). Two triple points appear, see *Figure 3.1*: one at the inner interface and the other at the outer interface.

The problem dynamics are characterized by the following dimensionless parameters

$$Pr = \frac{C_{pl}\mu_l}{k_l}, St = \frac{C_{pl}(T_m - T_c)}{L_h}, Bo = \frac{\rho_l g R^2}{\sigma}, Oh = \frac{\mu_l}{\sqrt{\rho_l R \sigma}} \quad (3.1)$$

$$R_{io} = \frac{R_i}{R_o}, \theta_0 = \frac{T_0 - T_c}{T_m - T_c}, \rho_{sl} = \frac{\rho_s}{\rho_l}, \rho_{gl} = \frac{\rho_g}{\rho_l}, \mu_{gl} = \frac{\mu_g}{\mu_l} \quad (3.2)$$

$$k_{sl} = \frac{k_s}{k_l}, k_{gl} = \frac{k_g}{k_l}, C_{psl} = \frac{C_{ps}}{C_{pl}}, C_{pgl} = \frac{C_{pg}}{C_{pl}} \quad (3.3)$$

To choose the grid resolution to use for the simulation, a hollow droplet solidifying on a cold surface with the parameters  $Pr = 0,01$ ,  $St = 0,1$ ,  $Bo = 0,1$ ,  $Oh = 0,01$ ,  $R_{io} = 0,5$ ,  $\rho_{sl} = 0,9$ ,  $\theta_0 = 1,0$ ,  $k_{gl} = 0,005$ ,  $\rho_{gl} = \mu_{gl} = 0,05$ ,  $k_{sl} = C_{psl} = 1,0$  và  $C_{pgl} = 0,24$ ,  $\phi_{0i} = \phi_{0o} = 90^\circ$  and  $\phi_{gr} = 0^\circ$  was performed. *Table 3.1* shows the mean error of height

Table 3.1. Mean error of  $128 \times 256$  grid compared to  $256 \times 512$  grid

Mean error (%)	128×256 grid compared with 256×512 grid	
	Height of the solidifying front	Height of the hollow droplet
	0,54%	0,22%

of solidification front and height of hollow droplet over time of two grids  $128 \times 256$  and  $256 \times 512$  for the  $3R \times 6R$  computational domain. It is seen that the mean error of the height of solidification front and the height of the hollow droplet of the  $128 \times 256$  grid compared with that of the  $256 \times 512$  grid is very small. In particular, the mean error of the height of solidification front of the  $128 \times 256$  grid compared with that of the  $256 \times 512$  grid is only 0,54%. Meanwhile, the mean error between these two grids is even lower for the hollow droplet height of only 0,22%. Since the two grids chosen for the simulation have a high degree of similarity, we can theoretically choose the  $128 \times 256$  grid. However, to give more accurate simulation results at the end of the solidification of the droplets, we choose the grid with a resolution of  $256 \times 512$  to simulate the problem.

The problem considers some main dimensionless parameters affecting the solidification of a hollow droplet on a cold surface such as  $Bo$  in the range of  $0,18 - 3,16$ ,  $Pr$  in the range of  $0,01 - 1,0$ ,  $St$  in the range of  $0,032 - 1,0$ ,  $\rho_{sl}$  in the range of  $0,8 - 1,2$ ,  $R_{io}$  in the range of  $0,2 - 0,7$  and the growth angle  $\phi_{gr}$  in the range of  $0^\circ - 25^\circ$ . Geometric parameters are also considered such as outer wetting angle  $\phi_{o}$  in the range of  $60^\circ - 130^\circ$  and inner wetting angle  $\phi_{i}$  in the



range  $50^\circ - 120^\circ$ . Other parameters are kept constant throughout the computation such as  $Oh = 0,01$ ,  $\theta_0 = 1,0$ ,  $k_{gl} = 0,005$ ,  $\rho_{gl} = \mu_{gl} = 0,05$ ,  $k_{sl} = C_{psl} = 1,0$  and  $C_{pgl} = 0,24$ .

### Conclusion of chapter 3

The main dimensionless parameters affecting the solidification of hollow droplets on a cold surface are investigated. Specifically, changing the thickness of the fluid shell by changing the radius of the gas bubble by varying the  $R_{io}$ , shows that increasing the size of the gas bubble leads to a longer time to complete solidification. While it does not affect the height of the hollow droplet at the end of solidification.

The height of the gas bubble inside of the solidified hollow droplet is not greatly affected by increasing  $Bo$  number (i.e., gravity plays a larger role than surface tension) in the range of  $0,18 - 3,16$  or  $St$  (i.e., reducing latent heat of fusion) in the range of  $0,032 - 1,0$ . However, increasing  $Pr$  (i.e., increasing the influence of momentum diffusion versus thermal diffusion) from  $0,01$  to  $1,0$  reduces the gas bubble height of the solidified hollow droplet. If we increase  $Pr$  and  $Bo$ , the height of the solidified hollow droplet will decrease.

The study on the change of solidification volume by changing the ratio of density of solid to liquid phases  $\rho_{sl}$ , showed that increasing the value of  $\rho_{sl}$  from  $0,8$  to  $1,2$  will reduce the height of the solidified hollow droplet and its gas bubble height. This leads to an earlier termination of solidification.

The effects of the geometric parameters (inner wetting angle ( $\phi_{oi}$ ) in the range  $50^\circ - 120^\circ$  and outer wetting angle ( $\phi_{oo}$ ) in the range

of  $60^\circ - 130^\circ$ ) and growth angle ( $\phi_{gr}$  in the range  $0^\circ - 25^\circ$ ) are also studied. Numerical simulation results show that when the inner wetting angle decreases and the outer wetting angle increases  $\phi_0 = 180^\circ - \phi_{0i} = \phi_{0o}$  and  $\phi_{gr} = 0^\circ$ , the height of the gas bubble and the outer droplet, and the solidification time increases, while, the height increment of the hollow droplet decreases after the solidification process ends. Similar effects were also investigated with an increase in the outer wetting angle (with  $\phi_{0i} = 90^\circ$  and  $\phi_{gr} = 0^\circ$ ). Increasing  $\phi_{0i}$  from  $50^\circ$  to  $120^\circ$  with  $\phi_{0o} = 90^\circ$  and  $\phi_{gr} = 0^\circ$  does not affect the outer droplet shape but results in an increase in the solidification time.

Solidification time, height and height increment of solidified hollow droplet as the growth angle increases. However, increasing the growth angle leads to a decrease in the height of the gas bubble after solidification is over. Besides, only  $\phi_{gr}$  affects the taper angle at the top of the outer droplet, i.e., increasing  $\phi_{gr}$  leads to a more conical outer surface. In other words, changing the outer and inner wetting angles, keeping  $\phi_{gr}$  constant, does not affect the tip angle.

*The results of chapter 3 have been published in 2 papers published in international journals in the list of SCIE (Q1), specifically, the papers number 1 and 2 in the "List of author's scientific works relating to the content of the dissertation"*

#### **CHAPTER 4. STUDYING THE PROCESS OF HEAT TRANSFER AND PHASE CHANGE OF A SUSPENDED HOLLOW FLUID DROPLET UNDER FORCED CONVECTION**

As mentioned in Chapter 3, hollow liquid droplets may solidify before reaching the cold surface as experimental works have shown. In this chapter, the problem of simulating phase change of such suspended hollow fluid droplets is performed.

Initially, we suppose that the spherical and symmetrical hollow droplet is suspended in a cold medium. The hollow droplet consists of a gas core (gas bubble or inner droplet) inside a fluid shell (outer droplet) that begins to solidify at a nucleus with radius  $r_0$  placed at the bottom of the droplet (*Figure 4.1*). The temperature of the nucleus is kept constant as  $T_c$ . Meanwhile,  $T_m$  stands for the phase change temperature of the fluid. The initial radii of the inner

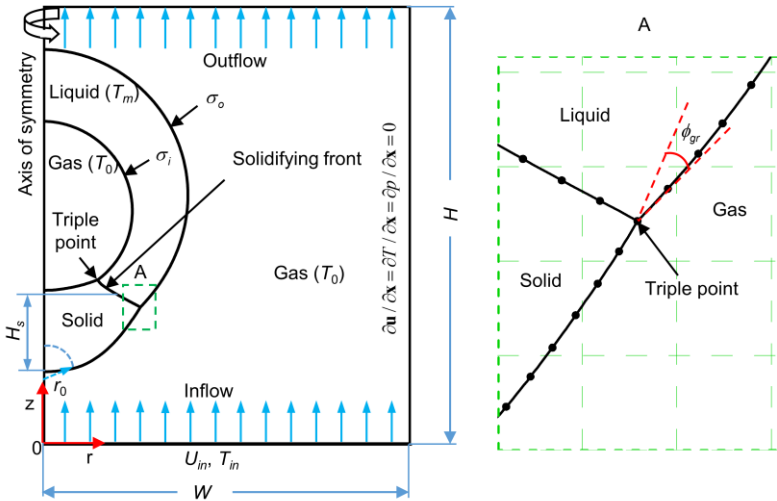


*Figure 4.1. Simulation problem model with half a symmetric hollow droplet suspended with a forced flow at the bottom of the computational domain*

and outer droplets are denoted as  $R_i = [3V_i/(4\pi)]^{1/3}$  and  $R_o = [3V_o/(4\pi)]^{1/3}$ , where  $V_i$  and  $V_o$  are the initial volumes of the inner and outer ones, respectively. At the bottom of the computational domain is a cold gas with temperature  $T_{in}$  and velocity  $U_{in}$ . To simplify the problem, we assume that  $T_{in}$  is equal to  $T_0$  – the initial temperature of the gas phase around the droplet. Unlike the solidification of a simple droplet, the hollow droplet has two triple points (*Figure 4.1*). There are three interfaces denoted as solid-liquid interface (i.e., solidification front), solid-gas interface and liquid-gas interface. In each phase, density ( $\rho$ ), viscosity ( $\mu$ ), thermal conductivity ( $k$ ) and heat capacity ( $C_p$ ) are also assumed to be constant.

The dimensionless parameters used in this problem are

$$Pr = \frac{C_{pl}\mu_l}{k_l}, St = \frac{C_{pl}(T_m - T_c)}{L_h}, Re = \frac{\rho_l U_{in} R}{\mu_l}, We = \frac{\rho_l U_{in}^2 R}{\sigma} \quad (4.1)$$

$$R_{io} = \frac{R_i}{R_o}, \theta_0 = \frac{T_0 - T_c}{T_m - T_c}, \rho_{sl} = \frac{\rho_s}{\rho_l}, \rho_{gl} = \frac{\rho_g}{\rho_l}, \mu_{gl} = \frac{\mu_g}{\mu_l} \quad (4.2)$$

$$k_{sl} = \frac{k_s}{k_l}, k_{gl} = \frac{k_g}{k_l}, C_{psl} = \frac{C_{ps}}{C_{pl}}, C_{pgl} = \frac{C_{pg}}{C_{pl}}, \varepsilon_0 = \frac{z_{ci0} - z_{co0}}{R} \quad (4.3)$$

To choose the grid resolution to simulate the problem, we investigate the grid convergence through considering 4 grid resolutions with the computational domain  $W \times H = 3R \times 12R$ :  $096 \times 384$ ,  $128 \times 512$ ,  $192 \times 768$  and  $384 \times 1536$ . The parameters are  $St = 0,1$ ,  $Pr = 0,01$ ,  $Re = 50$ ,  $We = 1$ ,  $\rho_{sl} = 0,9$ ,  $R_{io} = 0,6$ ,  $r_0/R = 0,2$ ,  $\varepsilon_0 = 0$ ,  $\theta_0 = 0$ ,  $\rho_{gl} = 0,05$ ,  $\mu_{gl} = 0,05$ ,  $k_{sl} = 0,5$ ,  $k_{gl} = 0,01$ , and  $C_{psl} = C_{pgl} = 1$ . *Table 4.1* shows the mean errors of the coordinates the radial

*Table 4.1. Mean error of different grids compared with  $384 \times 1536$  grid*

Mean error (%)	The different grids compared with $384 \times 1536$ grid		
	$096 \times 384$	$128 \times 512$	$192 \times 768$
Mean error of radial coordinate of the solidifying front	3,843%	2,973%	1,155%
Mean error of height of solidifying front	0,549%	0,410%	0,128%

coordinate and height of solidifying front of the different grids compared with the finest grid  $384 \times 1536$ . We see that the mean error of the  $192 \times 768$  grid compared with the  $384 \times 1536$  grid corresponds to the mean error of the radial coordinate of the solidifying front (1,155%) and the mean error of the height of the solidifying front (0,128%) is the smallest and these errors are acceptable. Therefore, to save computational resources and time while ensuring acceptable accuracy, a grid resolution of  $192 \times 768$  is chosen to study the problem.

In this chapter, some of the main dimensionless parameters affecting the solidification of a hollow droplet suspended in a cold medium are examined. Those parameters are  $Re$  in the range of 25-200,  $St$  in the range of 0,025 – 1,6,  $\rho_{sl}$  in the range of 0,8 – 1,2, nucleus size  $r_0/R$  in the range of 0,05 – 0,3, initial eccentricity  $\varepsilon_0$  in

the range of  $-0,15 - 0,3$ ,  $R_{io}$  in the range of  $0,2 - 0,7$  and growth angle  $\phi_{gr}$  in the range of  $0^\circ - 15^\circ$ . Other dimensionless parameters are kept constant during calculation such as  $Pr = 0,01$ ,  $We = 1$ ,  $\theta_0 = 0$ ,  $\rho_{gl} = 0,05$ ,  $\mu_{gl} = 0,05$ ,  $k_{sl} = 0,5$ ,  $k_{gl} = 0,01$ , and  $C_{psl} = C_{pgl} = 1$ .

### Conclusion of chapter 4

In this chapter, the solidification process of a suspended hollow droplet under the effect of forced convection has been presented. Parameters such as Reynolds number ( $Re$ ), Stefan number ( $St$ ), density ratio ( $\rho_{sl}$ ) between solid and liquid phase, solid core size ( $r_0/R$ ), initial eccentricity ( $\varepsilon_0$ ), radius ratio ( $R_{io}$ ) and growth angle ( $\phi_{gr}$ ) are considered.

Increasing  $Re$  (i.e., increasing the influence of inertia relative to the viscous force) in the range of  $25 - 200$ ,  $R_{io}$  (i.e., increasing the inner bubble size) in the range of  $0,2 - 0,7$  and  $\phi_{gr}$  in the range of  $0^\circ - 15^\circ$  leads to an increase in the solidification time ( $\tau_s$ ). In contrast, with a decrease in  $St$  (i.e., increase in latent heat of fusion) in the range of  $0,05 - 1,6$ ,  $r_0/R$  (i.e., decrease in nucleus size) in the range of  $0,05 - 0,3$  and  $\varepsilon_0$  (i.e., the gas bubble closer to nucleus) in the range of  $-0,15 - 0,3$  lead to a longer solidification process. Meanwhile, changing the density ratio between solid and liquid phases ( $\rho_{sl}$ ) in the range of  $0,8 - 1,2$  has a small effect on the solidification time.

The inner aspect ratio ( $Ar_i$ ) does not change much when the parameters are changed except for the change of  $\phi_{gr}$ . Accordingly, increasing the growth angle ( $\phi_{gr}$ ) reduces the inner aspect ratio ( $Ar_i$ ). Regarding the outer aspect ratio ( $Ar_o$ ), an increase in the density ratio

( $\rho_{sl}$ ) leads to a decrease in the outer aspect ratio ( $Ar_o$ ). On the other hand, the aspect ratio ( $Ar_o$ ) increases with increasing growth angle. Other parameters such as  $St$ ,  $Re$ , nucleus size ( $r_0/R$ ), initial eccentricity ( $\varepsilon_0$ ) of the droplet and the size of the gas bubble ( $R_{io}$ ) have little influence on the outer shape of the solidified hollow droplet.

*The main results of chapter 4 have been published in an international journal in the SCIE list (Q1), specifically, the paper number 5 in the "List of author's scientific works relating to the content of the dissertation"*

## CONCLUSION

The thesis has obtained the following main results:

1. The thesis has built a computational model of a hollow fluid droplet solidifying on a cold surface and a hollow fluid droplet suspended in a cold environment under forced convection are presented. These models have not been investigated in any other numerical simulation models.
2. Dimensionless parameters are given to investigate the solidification of a hollow fluid droplet on a cold surface. We see that, changing these parameters can lead to a change in the shape and solidification time of the droplets. Thereby, it is possible to control the solidification of hollow fluid droplets on a cold surface for industrial applications.

3. The solidification process of a hollow fluid droplet suspended in the cold environment under forced convection was also investigated. Thereby, it can be seen that the shape and solidification time of a hollow liquid droplet in a cold environment are also affected when the dimensionless parameters change. Therefore, investigating this effect can help to control the solidification process of hollow liquid droplets suspended in a cold environment.

## **NEW CONTRIBUTIONS OF THE DISSERTATION**

Solidification of simple fluid droplets has been accomplished through numerical simulations by the different methods. The works to simulate hollow fluid droplets have not been induced so far. Therefore, the thesis has the following new points:

- A computational model has been built of a hollow fluid droplet (i.e., compound liquid droplet) solidifying on a cold surface and a suspended hollow fluid droplet solidifying in the cold environment. Specifically, the gas bubble (inner droplet) is inserted inside the fluid droplet to form a model of a hollow fluid droplet. From there, an additional triple point appears at the inner boundary of the droplet;
- The influence of dimensionless parameters on the solidification of a hollow fluid droplet on a cold surface has been analyzed. Thereby, it is possible to adjust the



shape and solidification time of the hollow fluid droplet on a cold surface by adjusting the dimensionless parameters;

- The influence of dimensionless parameters on the solidification of a hollow fluid droplet suspended in a cold environment has been analyzed under forced convection. Adjustment of these dimensionless parameters causes a change in the shape and solidification time of the hollow fluid droplets suspended in the cold environment.

**LIST OF AUTHOR'S SCIENTIFIC WORKS RELATING TO  
THE CONTENT OF THE DISSERTATION**

1. Nang X. Ho, Truong V. Vu, **Binh D. Pham**, *A numerical study of a liquid compound drop solidifying on a horizontal surface*, International Journal of Heat and Mass Transfer, Vol. 165, nov. 2020, p. 120713 (SCIE, IF2020 = 5.584, Q1).
2. **Binh D. Pham**, Truong V. Vu, Lien V.T. Nguyen, Nang X. Ho, Cuong T. Nguyen, Hoe D. Nguyen, Vinh T. Nguyen and Hung V. Vu, *A numerical study of geometrical effects on solidification of a compound droplet on a cold flat surface*, Acta Mechanica, Vol. 232, jun. 2021, pp. 3767–3779 (SCIE, IF2020 = 2.698, Q1).
3. Truong V. Vu, **Binh D. Pham**, Phuc H. Pham, Hung V. Vu, and Bo X. Tran, *A numerical study of hollow water drop breakup during freezing*, Physics of Fluids, Vol. 33, oct. 2021, p. 112110 (SCIE, IF2021 = 4.98, Q1).
4. Truong V. Vu, **Binh D. Pham**, Nang X. Ho, Hung V. Vu, *Solidification of a hollow sessile droplet under forced convection*, Physics of Fluids, Vol. 34, Feb. 2022, p. 033302 (SCIE, IF2021 = 4.98, Q1).
5. **Binh D. Pham** and T. V. Vu, *A numerical study of a suspended compound droplet solidifying under forced convection*, Int. J. Heat Mass Transf, Vol. 196, p. 123296, Nov. 2022 (SCIE, IF2021 = 5.431, Q1).

6. **Pham Duy Binh**, Vu Van Truong, Nguyen Thi Viet Lien, Nguyen Tien Cuong, Nguyen Dinh Hoe, Nguyen Tuan Vinh, Vu Van Hung, *Direct numerical simulation study of water droplets freezing on a horizontal plate*, Vietnam J. Sci. Technol., vol. 59, no. 3, Art. no. 3, May 2021, doi: 10.15625/2525-2518/59/3/15434.

7. **Binh D. Pham**, Truong V. Vu, Lien V.T. Nguyen, Cuong T. Nguyen, Hoe D. Nguyen, Vinh T. Nguyen, Hung V. Vu, *A numerical study of the solidification process of a retracting fluid filament*, Vietnam J. Mech., Nov. 2021, doi: 10.15625/0866-7136/16393.